Central European Journal of Energetic Materials, **2009**, *6*(2), 149-165.
ISSN 1733-7178

Ageing Behaviour of HTPB Based Rocket Propellant Formulations

Sara CERRI[1, 2], Manfred A. BOHN[1], Klaus MENKE[1] and Luciano GALFETTI[2]

[1] *Fraunhoher Institut für Chemische Technologie (ICT)*
Postfach 1240, D-76318, Pfinztal-Berghausen, Germany
E-mail: sara.cerri@ict.fraunhofer.de

[2] *SPLab, Dipartimento di Ing. Aerospaziale,*
Politecnico di Milano 34 Via La Masa, I-20156 Milan, Italy

Abstract: The ageing of HTPB propellant formulations containing nanoAl is investigated. During natural ageing the material undergoes a series of slow physico-chemical degradation reactions. By using accelerated ageing conditions it is possible to simulate the material behaviour at different time-temperature conditions especially focused on the in-service conditions.
The mechanical and ageing behaviour of aluminised solid rocket propellants were investigated in terms of uniaxial tensile strength, DMA measurements, impact and friction sensitivity tests, SEM analyses.

Keywords: solid rocket propellant, HTPB, nanoAl, ageing, mechanical properties

Introduction

Composite solid rocket propellants consist of solid rigid fillers embedded in a rubbery polymeric matrix. During its in-service life, the material has to withstand different loads and environmental conditions. These boundary conditions can significantly alter the mechanical and ballistic properties. After the curing process of a solid composite propellant formulation many years can elapse before it will be used and the material will be naturally aged. During ageing the propellant undergoes different degradation processes that irreversibly change it. The mechanical properties of the propellant, the motor grain design (the shape of the grain and the web thickness), the operational and environmental conditions and the ageing characteristics of the material determine the amount of degradation. The ageing of the propellant can be caused by several processes:

- Chemical processes as oxidative cross-linking, chain scission by hydrolysis and consecutive reactions following oxidative attack, antioxidant depletion, binder oxidation;
- Physical processes as plasticiser depletion and migration, humidity, presence of liquid burn catalyst (depletion by migration), phase transition, dewetting;
- Mechanical processes as vibration, thermal slump, thermally induced stresses during temperature changes.

The first two processes are related to the molecular reactions and diffusion phenomena which are governed by kinetic processes. They can be accelerated by increasing the temperature. Oxidative phenomena are introduced already during manufacturing at the kneading and at the curing of the formulation, in spite of the presence of antioxidants. That means some oxidative pre-damaging has already occurred after the curing process. With time, these defects and pre-damages can evolve to create micro-fractures and macro-fractures and lead to unacceptable deviations. So, in order to simulate the long-term ageing within a reasonable time period, motors or propellant specimens are aged at temperatures higher than ambient temperature. The common method for predicting the in-service time of the propellant involves the use of the Arrhenius equation which states that the equivalent usetime at any accelerating temperature is proportional to $\exp(-E_a/R\cdot T)$, where E_a is the activation energy for the physico-chemical process in consideration, R is the general gas constant, T is the absolute temperature in K. With this approach it is possible to predict the behaviour of the material with data obtained in short experimental times. The hypothesis in applying the Arrhenius approach is that the chemical processes occurring at the accelerating temperature exposures and those that occur under the natural ageing are identical. Unfortunately, the assumption is not always fulfilled and the extrapolated information may not match the changes observed during natural ageing.

The task of an accelerated ageing programme is to understand and evaluate the degree to which the propellant degradation is accelerated by increasing the temperature since this relationship is necessary to design the accelerated ageing test protocols for the determination of the motor service time period. Different researchers have done analyses on the ageing behaviour of solid propellants [1-4]. It was found that the change of some mechanical properties as tensile strength and strain at break can be more or less satisfactorily described by the following empirical relation:

$$\left.\left(\frac{dP(t,T)}{dt}\right)\right|_T = \frac{S_p(T)}{t} \tag{1}$$

P = property at the time t (usually it is a mechanical property); S_p = scaling parameter; T = ageing temperature.

The integration of the Eq.(1) gives:

$$P(t,T) = P_0(t_0) + S_p(T)\cdot c\cdot \log\left(\frac{t}{t_0}\right) \tag{2}$$

P_0 = property at the time t_0; t_0 = referred time at start (e.g. some time after curing); c = ln(10).

With the use of Eq. (2) it is possible to extrapolate the behaviour of the material and predict the values at long ageing time. By assuming that one of the propellant property P assumes the same value after a time t_a by the accelerated ageing, and after a time t_n by natural one, $P(t_a,T_a) = P(t_n,T_n)$ and $P_0(t_0,T_a) = P_0(t_0, T_n)$, the previous equation can be rewritten as:

$$t_n(T_n) = t_0\cdot\left(\frac{t_a(T_a)}{t_0}\right)^{\frac{S_p(T_a)}{S_p(T_n)}}. \tag{3}$$

This relationship, also called Layton model [1], correlates accelerated and natural ageing in order to predict the in-service time of the propellant. Note that the parameter k mentioned in the Layton model is not a rate constant. It is a dimensionless quantity and it is equal to the parameter named here s.

To define an ageing programme in terms of time-temperature load data one can use an empirical formula [5], applicable for ageing processes based on chemical reactions, Eq. (4).

$$t_E[y] = t_T[d]\cdot F^{\frac{T_T - T_E}{\Delta T_F}}\cdot\frac{1}{365.25} \tag{4}$$

t_E = time in years at the in-service temperature T_E; t_T = test time in days at the test temperature T_T; F = reaction rate change factor per 10 °C of temperature change, usually between 2 and 5; ΔT_F = temperature interval for actual value of F (10 °C was used here only). T_T and T_E are both in °C.

The value of the scaling factor F is a function of the activation energy (E_a) of the ageing process, e.g. with activation energy values of about 80 to 120 kJ/mol and a temperature range between 20 °C and 90 °C the scaling factor is about 3. Consumption of antioxidant and oxygen uptake shows activation energies in the range from 90 to 130 kJ/mol, this means a factor 3 could be applied. But here a scaling factor of 2.5 was taken to establish the ageing plan. This gives a conservative description, which means the accelerated ageing is done at longer times than those calculated with factor F=3. Using Eq.(4) with a scaling factor equal to 2.5 a thermal accelerated ageing programme was carried out in PID temperature-controlled (± 0.5 °C) ageing ovens (design based on former company Julius Peters, Berlin). The aim of the study was the evaluation of the accelerated ageing of the surface-layer of solid rocket propellants (no "in core" analyses), so specimens were aged at 60 °C (75, 150, 220 days), 70 °C (30, 60, 90 days), 80 °C (12, 25, 40) and 90 °C (5, 10, 15 days) in air (RH<10%) to simulate 15 years of natural ageing at 25 °C.

Formulations

Several aluminised HTPB/AP-based propellant formulations were investigated. AP means ammonium perchlorate. The propellants have been divided into two groups in order to study the influence of the filler content and of the average size of the particles: the odd-numbered propellants named AV03 and AV05 contain the 6 mass-% of aluminium, while the even-numbered propellants named AV04 and AV06 contain 12 mass-% Al. Propellants AV03 and AV04 have micrometric aluminium of 18 μm (Grade X-81, Lot. SI 23289, Eckart, Austria). Propellant AV05 has only nanometric aluminium inside (ALEX, 100-200 nm, USA), AV06 has a 6 mass-% of nanoAl and a 6 mass-% of microAl. Table 1 shows the formulations. All the formulations were prepared in a vertical kneader (Drais T FHG, Germany) having a volume of 5 l and cured in an electrical oven cabinet (from company Memmet, Germany) for two days at 60 °C.

Table 1. Compositions of the propellant formulations in mass-%

Components	AV03, m-%	AV04, m-%	AV05, m-%	AV06, m-%
AP	78	72	78	72
Al	6	12	6	12
HTPB R45M™	10.72	10.72	10.72	10.72
DOA	4	4	4	4
HX-878	0.19	0.19	0.19	0.19
Irganox™ 565	0.2	0.2	0.2	0.2
IPDI	0.89	0.89	0.89	0.89
Triphenylbismuth	0.02	0.02	0.02	0.02

TM = Trade Mark

The propellants are highly-filled with particles of oxidizer (AP) and fuel (Al), so the binder must have a sufficiently low viscosity in order to wet the particles, to achieve a homogeneous mix, and to be fluid enough to fill moulds completely. The EOMV (end of mix viscosity) increases by adding nano-sized aluminium particles [6, 7]. In order to avoid too high EOMV, the fraction of nanoAl inserted into the material was limited to 6 mass-%.

Evaluation of the ballistic performances

The ballistic performances of the propellant formulations were calculated using the ICT-Thermodynamic code together with the ICT Thermochemical Database. The thermodynamic equilibrium in the nozzle was calculated at constant pressure with the expansion ratio of 70:1 according to EU standard conditions. The gravimetric specific impulse (I_{sp}), the volumetric specific impulse (I_{spv}) and the vacuum specific impulse ($I_{spvacuum}$) were calculated for two conditions: frozen equilibrium and equilibrium flow. The calculations were performed using the same binder fraction (16 mass-%) and making an aluminium content sweep (increasing the amount of Al and accordingly decreasing the amount of AP) from 0 mass-% to 18 mass-%. The aluminium particles are covered with an amorphous oxide layer of alumina (Al_2O_3) having a thickness of approximately 3-4 nm. The variations in the parameters of interest caused by different particle size can be evaluated by considering the active aluminium content (Al^0) of the metal particles it is possible to evaluate the variations in the parameters of interest caused by different particle size. Table 2 shows the values considered.

Table 2. Composition of the Al particles in aged and unaged conditions

Composition of the Al particles, mass-%	Unaged conditions		Aged conditions	
	µAl	nAl	µAl	nAl
Al^0	99.6	88.2	72.5	4
Al_2O_3	0.4	11.8	0.4	11.8
$Al(OH)_3$	0	0	27.1	84.2

The use of the nanopowders could lead to some problems. Nanopowders are very susceptible to ageing phenomena. Under strong accelerated ageing conditions (high temperature and high relative humidity) the powders degrade rapidly. The reaction with moisture produces bayerite ($Al(OH)_3$) rather than Al_2O_3 [6, 8, 9]. Therefore the ageing behaviour of the aluminium powders was also taken into account in order to understand what happens from the thermochemical point of view. Thus, in order to have more representative thermochemical calculations, the values of active aluminium content published in the paper of Cliff et al. [8] for unaged and aged micrometric and nanometric particles were used. The value of the aluminium content after ageing of the nanometric powders agrees with the results obtained by Brousseau et al. [10]. The performance calculations were done by varying the active aluminium fraction in the material. The alumina content after ageing was kept constant, which implies that the decrease in the aluminium content has formed only bayerite. The active aluminium, the alumina and the bayerite fractions are listed in Table 2.

Experimental techniques

The unaged propellants have been tested with the ZWICK UPM 1476 tensile test machine. JANNAF dog bone samples (125 mm length, 25 mm width, 10-12 mm thickness) were used in uniaxial tensile tests at room temperature and atmospheric pressure at three constant crosshead speeds: 5, 50, 500 mm/min. Dividing the crosshead speed by the effective gauge length of the JANNAF sample (50 mm) the values of the strain rates are obtained: 0.00167 s^{-1}, 0.0167 s^{-1}, 0.167 s^{-1}. During each test the applied load and the displacement were recorded.

Scanning electron microscopy (SEM) and energy dispersive X-ray (EDX) analyses were performed using the scanning electron microscope Supra 55 VP manufactured by ZEISS, Germany. Pieces of propellant (10x10x10 mm) were cut out from the JANNAF dog bone of the unaged material after the tensile tests. SEM analyses were undertaken for all the crosshead speeds applied whereas the EDX analyses were made only with material subjected to the crosshead speed of 500 mm/min.

The dynamic mechanical measurements were carried out using a DMA instrument of type ARES (Advanced Rhemoetric Expansion System) manufactured by former Rheometric Scientific Inc. Piscataway, New Jersey, USA (now belonging to Waters, Inc, BU TA Instruments) in the torsion mode. A liquid-nitrogen cooling accessory was used for the low and high temperature operations. The samples were small rectangular bars with the dimensions of 10 mm wide, 4 mm thick and 50 mm long. The temperature range was -100 °C to 70 °C, with the heating rate of 1 °C/min and the soak time of 28 s. The specimens were tested at four frequency values (0.1, 1.0, 10.0, 56.0 Hz) using a strain control with maximum strain of 0.0012. The measurement reproducibility is very high so only one sample per each testing condition was tested. In the case of anomalous behaviour a second measurement was performed.

DSC analyses were performed in nitrogen atmosphere using the DSC 2920 manufactured by TA Instruments. Small amounts of propellants (of the order of 10 mg) were analysed with a heating rate of 10 °C/min, starting from -120 °C and ending at room temperature. These analyses were done for the unaged and aged material.

Impact sensitivity and friction sensitivity were determined according to BAM (Bundesanstalt für Materialforschung und Materialprüfung, Berlin, Germany) procedures with the BAM-Impact sensitivity tester and the BAM-Friction sensitivity tester made by the former company Julius Peters (Berlin, Germany). The values reported are the smallest load under which deflagration has been noted at least one time in six consecutive tests. The effect of the ageing at 90 °C on impact and friction sensitivity was investigated. The quantities determined are named: limit impact energy (N·m or J) and limit friction force (N).

Results and Discussion

Ballistic performance using the ICT-Thermodynamic code

A parametric study by varying the Al content from 0 mass-% to 18 mass-% (binder was 16 mass-%) was done in order to quantify the influence of the ageing on the performance of the propellants. Three cases were analysed: propellant containing only micrometric aluminium, propellant with only nanometric Al and propellant having a mixture of nanoAl and microAl, 50% and 50% respectively.

The propellant formulations containing unaged aluminium show an increase in the ballistic performance by adding more metal inside the mixture (Figure 1). Micrometric powders have the highest Al^0 content, therefore the propellants containing microAl have also the highest ballistic quantities. Then the mixture and the nanopowders follow with regard to the values of the ballistic quantities. From a thermodynamic point of view it is not advantageous to use the nanoAl because it has a higher content of aluminium oxide (Table 3).

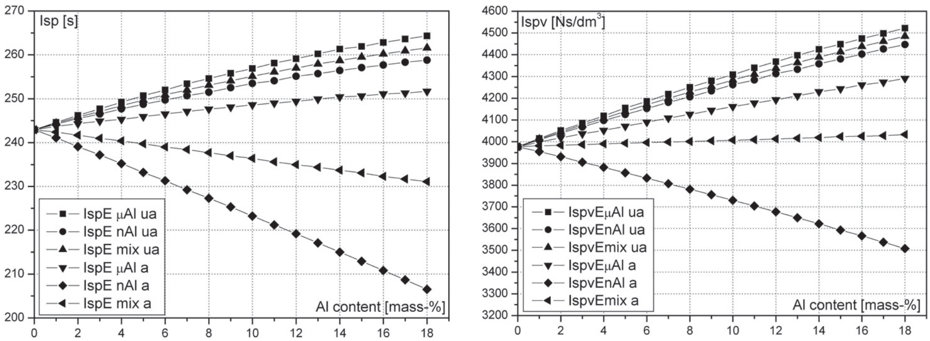

a) b)

Figure 1. a) Gravimetric impulse I_{sp} vs. solid filler of formulations containing aged and unaged aluminium powder; b) Volumetric impulse I_{spv} vs. solid filler of formulations containing aged and unaged aluminium powder.

Table 3. Active aluminium content of the unaged AV formulations

Propellants	Al content, mass-%	Type of Al	Al^0, mass-%	Al_2O_3, mass-%
AV03	6	only μm	5.976	0.024
AV05	6	only nm	5.292	0.708
AV04	12	only μm	11.952	0.048
AV06	12	6 mass-% nm + 6 mass-% μm	11.268	0.732

For the propellants containing aged material the behaviour among the three model-formulations is completely different. The material having aged microAl shows again an increase of the performances with the Al fraction. The trend of the gravimetric specific impulse and of the volumetric specific impulse of the material containing the mixture of Al or only the nanoAl is similar; they show a decrease in the ballistic performance with increasing the aluminium fraction because there is an increase of the inert masses (Al_2O_3 and $Al(OH)_3$). The losses in performance with formulations having only nanoAl are significant. From a thermodynamic point of view, the use of nano aluminium particles leads to reductions of the interesting parameter values. By using them the gravimetric specific impulse looses about 20 s for both formulations.

Table 4. Parameters calculated by the ICT thermochemical code

Propellants	AV03	AV05	AV04	AV06
Oxygen balance, %	-26.49	-25.88	-33.85	-33.24
Density, g/cm^3	1.693	1.696	1.718	1.721
$I_{sp\ frozen}$, s	249.3	247.3	256.3	254.6
$I_{sp\ equil}$, s	252.0	249.8	259.1	257.2
$I_{spvacuum\ frozen}$, s	268.6	266.4	277.1	275.2
$I_{spvacuum\ equil}$, s	272.2	269.7	281.0	278.8
$I_{spv\ frozen}$, N·s/dm^3	4141	4113	4320	4297
$I_{spv\ equil}$, N·s/dm^3	4186	4155	4367	4341
$T_{chamber}$, K	2967.5	2925.8	3146.2	3108.2

By increasing the fraction of Al metal the I_{sp}, I_{spv} and $I_{spvacuum}$ increase (Table 4). The problem is that with ageing the fraction of the active aluminium is reduced (Table 5), leading to a decrease in the performance values (Table 6). By using micrometric aluminium these losses are about 2% for the propellant having an aluminium fraction of 6 mass-% and 4% for the propellant having an aluminium fraction of 12 mass-%. With nanoAl these losses become significant: around 7% by using only nanoAl (6 mass-%) and about 8% by using a mixture of nanoAl and microAl. The resulting reduction in the combustion temperature of the material containing nanopowders is high: 13.2% for AV05 and 15.58% for AV06. This has important consequences on the efficiency of the combustion process. The calculations performed underline the importance of the storage conditions and the quality of the motor sealing especially for motors containing nano-sized powder.

Table 5. Active aluminium content of the aged AV formulations

Propellants	Al content, mass-%	Type of Al	Al^0, mass-%	Al_2O_3, mass-%	$Al(OH)_3$, mass-%
AV03	6	All µm	4.35	0.024	1.626
AV05	6	All nm	0.24	0.708	5.052
AV04	12	All µm	8.70	0.048	3.252
AV06	12	6 mass-% nm 6 mass-% µm	4.59	0.732	6.678

Table 6. Compilation of the losses in the parameters values using aged aluminium inside the formulations

Propellants	AV03, %	AV05, %	AV04, %	AV06, %
$I_{sp\ frozen}$, s	1.97	7.04	3.43	8.01
$I_{sp\ equil}$, s	2.18	7.41	3.74	8.48
$I_{spvacuum\ frozen}$, s	2.05	7.21	3.57	8.32
$I_{spvacuum\ equil}$, s	2.28	7.71	3.99	8.93
$I_{spv\ frozen}$, N·s/dm³	2.08	7.34	3.66	8.45
$I_{spv\ equil}$, N·s/dm³	2.29	7.75	3.98	8.91
$T_{chamber}$, K	3.89	13.20	6.96	15.58

Tensile strength

The thermo-viscoelastic behaviour of the propellants was characterised in terms of corrected stress and logarithmic strain. By increasing the strain rate the strength, stiffness and the strain capability of the unaged materials increase.

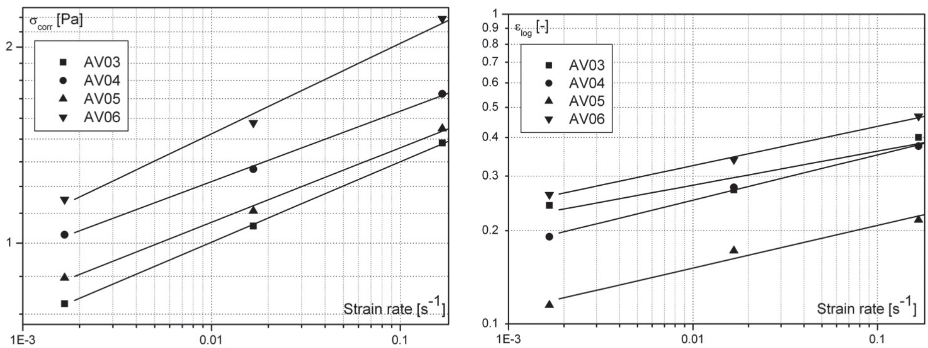

a) b)

Figure 2. a) Bi-logarithmic plot of the corrected stress vs. the strain rate; b) Bi-logarithmic plot of the logarithmic strain vs. the strain rate.

The AV-even-numbered propellants containing the 12 mass-% of aluminium achieved higher strength values. Figure 2 shows a linear trend of two of the previous cited quantities plotted in bi-logarithmic graphs. The use of nanoAl gives higher strength with respect to the use of micrometric aluminium. The strength of the material is influenced by the morphology and the average diameter of the powders. Decreasing the size, so increasing the specific surface of the powders the propellants reach higher strength. The performed analyses indicate that in order to achieve good mechanical properties it is better to use not only nanoAl but a mixture of nanoAl and spherical microAl.

EDX and SEM analyses

Figure 3 shows the SEM micrographs and the EDX mapping of aluminium. SEM images evidence the morphology of the material and the absence of micro-voids and dewetting phenomena. The last item therefore underlines the effectiveness of the bonding agent used. EDX mapping micrographs clearly show that the propellants containing nanoAl have a high dispersion level of the aluminium particles. The size of the powder is so small that the powder is able to mix homogeneously within the matrix.

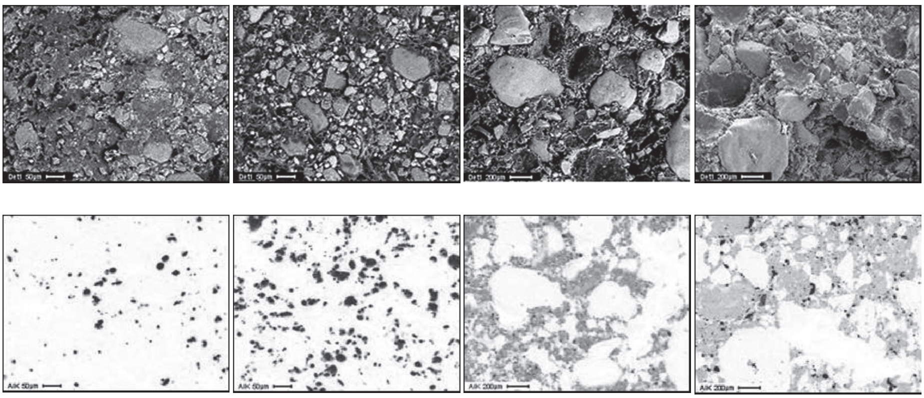

a) b) c) d)

Figure 3. SEM and EDX analyses of the unaged propellants tested with a uniaxial test at 500 mm/min: a) AV03; b) AV04; c) AV05; d) AV06.

Further the EDX mapping made at high magnification has revealed also the presence of nearly perfect spherical micrometric aggregates of nanoparticles having an average diameter of 2 μm (Figure 4), formed during the kneading. Therefore the reduction in performance due to the marked decrease of the specific surface of the metal particles used has to be taken into account.

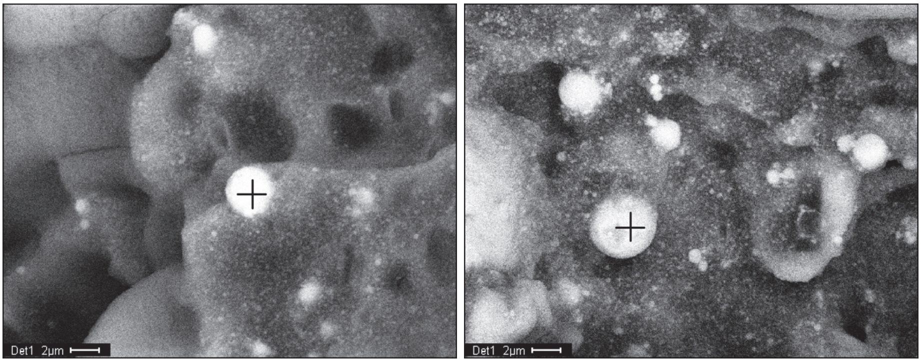

a) b)

Figure 4. EDX analysis at high magnification for: a) propellant AV05; b) propellant AV06.

DMA measurements

Before the ageing study an investigation of the mechanical properties of the unaged propellants has been done to get the baseline data. Figure 5 shows the storage modulus (log(G')), the loss modulus (log(G'')), the loss factor (tan(δ)) as function of temperature.

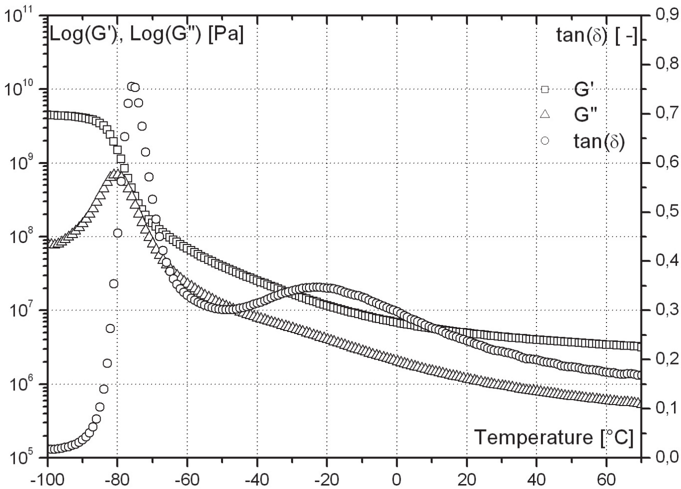

Figure 5. Log(G'), Log(G'') and tan(δ) of the unaged AV06 propellant as function of temperature at a frequency of 1 Hz.

Two maxima in the loss factor curve can be seen. The first is located between -80 °C and -60 °C (depending on frequency) and is attributed to the main glass transition temperature in the soft-segment regions (HTPB main chain elements) where the main chain molecular motion ceases or starts. At this temperature range a molecular rearrangement occurs and it is defined as the temperature at which the polymeric material changes from the entropy-elastic rubber behaviour to the energy-elastic glass behaviour. This temperature will be called $T_g^{unrestricted}$. The values of $T_g^{unrestricted}$ agree with that found by DSC measurements. The value of $T_g^{unrestricted}$ is frequency dependent and can be parameterized by Eq. (5).

$$f = f_0 \cdot \exp\left(-\frac{E_a}{R \cdot T}\right). \tag{5}$$

f = applied deformation frequency; f_0 = pre-exponential factor of deformation frequency; E_a = pseudo activation energy in kJ/mol; R = gas constant, 8.31441 J/K/mol; T = absolute temperature, in K.

The second maximum in tan(δ), which is also frequency dependent, is broader than the first peak and it appears at much higher temperature. It can be related to the motions within short hard-segments units or mobility restricted soft-segment regions. This process is referred to as the glass transition of the mobility restricted segments ($T_g^{restricted}$) and it is assumed to be related to the filler-binder interactions [11-14]. The shift of the temperature in the relaxation maxima with frequency allows the estimation of the apparent activation energy of the distinct relaxation (molecular transformation) phenomena. The different nature of the two observed relaxation mechanisms is reflected in the values of E_a. The apparent activation energy of the process associated with the cooperative motions of long soft segments ($T_g^{unrestricted}$ process) is higher (150-170 kJ/mol) than that associated with the motions in by filler-matrix interactions mobility restricted segment (70-80 kJ/mol). The value of the apparent activation energy of the first peak seems to be influenced by the presence of different amount of metal filler (see AV03 vs. AV04 and AV06) and by the presence of nanoAl (see AV03 vs. AV05) as shown in Table 7.

Table 7. Apparent activation energy evaluation of the first and second peak of the unaged propellants

Apparent activation energy	AV03	AV05	AV04	AV06
$E_a(T_g^{unrestricted})$, kJ/mol	149	172	164	165
$E_a(T_g^{restricted})$, kJ/mol	76	77	73	77

Regarding the first peak, the behaviour of the aged and unaged material is quite similar, Figure 6. However, the changes are remarkably considering the second peak. The values of tan(δ) are reduced with the ageing time. The area under the curve decreases. This area is related to the ability of the material to dissipate energy during rearrangement. One interpretation of this reduction is related to an increase in the material stiffness due to, probably, the oxidative cross-linking. Also a decrease in filler-binder interaction is possible, thereby this part of binder is released and its response moves towards the unrestricted binder. The heights of the first peak and the second peak were influenced by the composition. Propellants containing nanoAl have shown the highest loss factor in the first peak that means a more viscous behaviour. In molecular terms this means more dissipation of introduced deformation energy by molecular rearrangement activities. In the second peak AV06 has the lowest value.

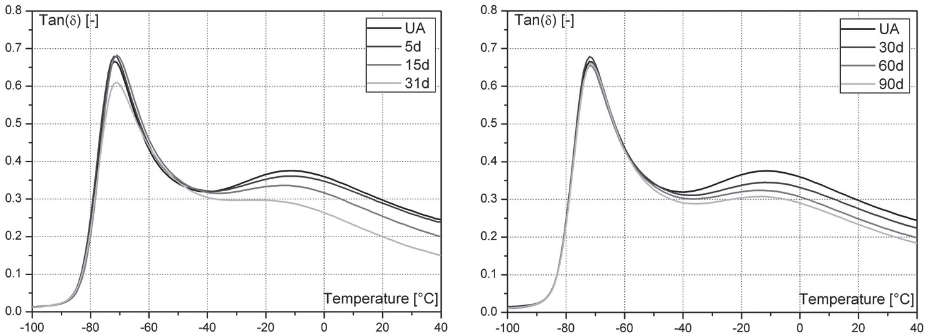

a) b)

Figure 6. a) Loss factor vs. Temperature for the propellant AV04 aged at 90 °C; b) Loss factor vs. Temperature for the propellant AV04 aged at 70 °C.

DSC measurements

With the thermal accelerated ageing no differences in the values of the glass transition temperature are observed (Table 8). This result underlines the good effectiveness of the antioxidant used.

Table 8. Glass transition temperature evaluated for unaged and aged propellants

Propellant	$T_g^{unrestricted}$ unaged material, °C	$T_g^{unrestricted}$ aged material, °C
AV03	-83.05	-82.93
AV04	-82.87	-82.93
AV05	-81.67	-83.71
AV06	-82.14	-83.11

Impact and friction sensitivity

The friction sensitivity of the propellants increases by using small size aluminium powders [6]. From looking at all the data sets (Figure 7) the overall trend is that the samples become more friction sensitive by ageing. Regarding the impact sensitivity, small influences of the av-erage diameter of the aluminium powders may be recognized. Considering the general trend, however, propellants are not influenced by ageing, especially those containing only micromet-ric aluminium. The variation in the data was typical of what can be expected for the test method.

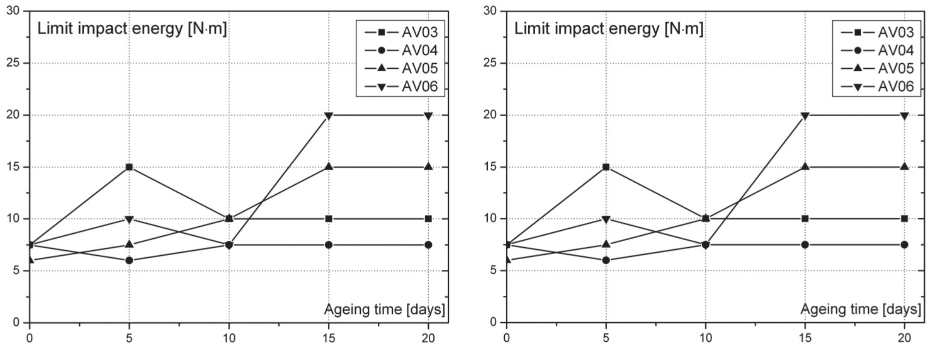

a) b)

Figure 7. a) Ageing behaviour of the impact sensitivity expressed as the limit impact energy values according to BAM method; b) Ageing behaviour of the friction sensitivity expressed as the limit friction force values according to BAM method.

Conclusions

HTPB/AP-based propellant formulations were investigated in order to study the influence of the filler content and of the average size of the particles (nanometric vs. micrometric Al) on the mechanical properties and on the ageing behaviour. The thermochemical calculations have shown that propellants containing unaged micrometric aluminium show an increase in the ballistic performance results by adding more metal inside the mixture because this powder has a high Al^0 content and the increases are higher than for propellant containing only nanoAl. Consequently, from a thermodynamic point of view it is not convenient to use nanoAl because it has a lower content of Al^0. Nanopowders are significantly susceptible to ageing phenomena and under strong accelerated ageing conditions degrade rapidly. The material having aged microAl shows again an increase of the performances with the Al fraction. However, for the mixture of nano and micro Al and the propellants containing only nanoAl the trend is opposite. The calculations have underlined the importance of the storage conditions and of the quality of the motor sealing.

By increasing the strain rate the strength, stiffness and the strain capability of the material increase. The AV-even-numbered propellants achieve higher strength values. The strength of the material is influenced by the morphology and the average diameter of the metal powders. Increasing the specific surface of the powders the propellants reach higher strength.

The propellants containing nanoAl have a high dispersion level of the Al particles. But actually the EDX mapping made at high magnifications showed the presence of perfectly spherical micrometric aggregates. This behaviour leads to a reduction in the performance of the propellants due to the significant decrease of the specific surface of the metal particles.

DMA measurements have revealed the presence of two peaks in the loss factor curve. The first is associated with the main glass transition temperature in the region where the main chain molecular motion ceases or starts. The second peak, broader than the first one and located at higher temperatures, is related to the movements of chains in the zone of binder-filler interactions. The evaluation of the apparent activation energy for the first peak seems to be influenced by the presence of different amount of metal filler and by the presence of nanoAl. The behaviour of the first peak is quite similar for the aged and unaged material. The changes are remarkable considering the second peak. The values of tan(δ) are reduced with the ageing time.

DSC measurements could not reveal differences in the value of the glass transition temperature with ageing.

The friction sensitivity of the propellants increases by using small particle size aluminium powders. The overall trend was some increase in friction sensitivity by ageing. The impact sen-sitivity values are less influenced by the average diameter of the aluminium powders. More-over, the trend is not influenced by ageing, especially for propellants containing only micro-metric aluminium.

References

[1] Layton L.H., Chemical structural aging studies on an HTPB propellant, AFRPL-TR-75-13, **1975**.

[2] Lillo F., D´Andrea B., Marcelli G., Sebasta A., Long Term Aging of Aerospace and Tactical SRM. Experimental Study, *37th AIAA/ASME/SAE/ASEE Joint Propulsion Conference and Exhibit*, 8-11 July, Salt Lake City, Utah, **2001**, AIAA Paper 2001-3284.

[3] Sbriccoli E., Salterelli R., Martinucci S., Comparison between Accelerated and Natural Aging, *20th International Annual Conference of ICT* and *18th Annual Technical Meeting of GUS*, 27-30 June, Karlsruhe, Germany, **1989**.

[4] Kivity M., Hartman G., Achlama A.M., Aging of HTPB Propellant, *41st AIAA/ASME/SAE/ASEE Joint Propulsion Conference and Exhibit*, 10-13 July, Tucson, Arizona, **2005**, AIAA Paper 2005-3802.

[5] Bohn M.A., Prediction of Equivalent Time-Temperature Loads for Accelerated Ageing to Simulate Preset In-Storage Ageing and Time-Temperature Profile Loads, *40th International Annual Conference of ICT*, 23-26 June, Karlsruhe, Germany, **2009**, paper 78.

[6] Shalom A., Aped H., Kivity M., Horowitz D., The Effect of Nanosized Aluminum on Composite Propellant Properties, *41st AIAA/ASME/SAE/ASEE Joint Propulsion Conference and Exhibit*, 10-13 July, Tucson, Arizona, **2005**, AIAA Paper 2005-3604.

[7] Bui D.T., Atwood A. I., Atienzamoore T.M., Effect of Aluminum Particle Size on Combustion Behavior of Aluminized Propellants in PCP Binder, *35th International Annual Conference of ICT*, 29 June-2 July, Karlsruhe, Germany, **2004**, paper 27.

[8] Cliff M., Tepper F., Lisetsky V., Ageing Characteristics of Alex® Nanosize Aluminum, *37th AIAA/ASME/SAE/ASEE Joint Propulsion Conference and Exhibit*, 8-11 July, Salt Lake City, Utah, **2001**, AIAA Paper 2001-3287.

[9] Meda L., Marra G., Galfetti L., Severini F., DeLuca L.T., Nano-aluminum as energetic material for rocket propellants, *Material Science and Engineering C*, **2007**, *27*, 1393-1396.

[10] Brousseau P., Crête J.P., Dubois C., Ageing of Polymer-Coated Ultra-Fine Particles, *36th International Annual Conference of ICT* and *32nd International Pyrothecnics Seminar*, 28 June-1 July, Karslruhe, Germany, **2005**, paper 89.

[11] de la Fuente J.L., Fernández-García M., Cerrada M.L., Viscoelastic Behavior in a Hydroxyl-Terminated Polybutadiene Gum and Its Highly Filled Composites: Effect on the Type of Filler on the Relaxation Processes, *Journal of Applied Polymer Science*, **2003**, *88*, 1705-1712.

[12] de la Fuente J.L., Rodrìguez O., Dynamic Mechanical Study on the Thermal Aging of a Hydroxyl-Terminated Polybutadiene-Based Energetic Composite, *Journal of Applied Polymer Science*, **2003**, *87*, 2397-2405.

[13] Ramier J., Gauthier C., Chazeau L., Stelandre L., Guy L., Payne Effect in Silica-Filled Styrene-Butadiene Rubber : Influence of Surface Treatment, *Journal of Polymer Science : Part B : Polymer Physics*, **2007**, *45*, 286-298.

[14] Tsagaropoulus G., Eisenberg A., Dynamic Mechanical Study of the Factors Affecting the Two Glass Transition Behavior of Filled Polymers. Similarities and Differences with Random Ionomers, *Macromolecules*, **1995**, *28*, 6067-6077.